Chung et al. Int J Concr Struct Mater (2018) 12:78
https://doi.org/10.1186/s40069-018-0313-0

International Journal of Concrete Structures and Materials

RESEARCH

Open Access

Performance Evaluation of CFRP Reinforced Concrete Members Utilizing Fuzzy Technique

Lan Chung, Moo-Won Hur and Taewon Park*

Abstract

Aging and structural deterioration under severe environments are major causes of damage in reinforced concrete (RC) structures, such as buildings and bridges. Degradations such as concrete cracks, corrosion of steel, and deformation of structural members can significantly degrade the structural performance and safety. Therefore, effective and easy-to-use methods are desired for repairing and strengthening such concrete structures. Various methods for the strengthening and rehabilitation of RC structures have been developed over the past several decades. Recently, FRP composite materials have emerged as a cost-effective alternative to conventional materials for repairing, strengthening, and retrofitting deteriorating/deficient concrete structures, by externally bonding FRP laminates to concrete structural members. The main purpose of this study is to investigate the effectiveness of the FRP retrofit for circular type concrete columns under the framework of the adaptive neuro-fuzzy inference system (ANFIS). Retrofit ratio, strength of existing concrete, thickness, number of layer, stiffness, ultimate strength of fiber, and size of specimens are used as input parameters to predict strength, strain, and stiffness of the post-yielding modulus. These proposed ANFIS models show reliable increased accuracy in predicting the constitutive properties of concrete retrofitted by FRP, compared to the constitutive models suggested by other researchers.

Keywords: adaptive neuro-fuzzy inference system, FRP retrofitting, compressive concrete strength, strain, 2nd elastic modulus

1 Introduction

The performance of concrete structures needs to be improved to compensate the deterioraton induced by adverse environment, inadequate maintenance, or spontaneously varied natural conditions. The application of sectional augmentation or steel plate attachment employed to column elements has limitations due to the increase of dead weight to foundations and reduced usability. In contrast, the method employing FRP materials has been broadly propagated, because it enables comparatively simple construction work that could secure the integrity of concrete structures. Due to its advantages of excellent reinforcement effects together with superior durability and corrosion resistance realizable in a rather short construction period, the FRP materials have been broadly employed in recent maintenance and reinforcement works (Al-Nimry and Ghanem 2017).

Richart (1928) et al. conducted a study to improve the strength (of concrete members) through the lateral binding of concrete, whale Mander et al. (1988) demonstrated the effect of lateral binding through their study that mathematically examined the stress–strain relationship of laterally bound concrete; thereafter, researchers have developed the design formulae of laterally bound concrete with the development of diverse kinds of fibers.

Lee et al. (2007) and Cho (2007) also conducted tests to predict the strength and strain of the concrete retrofitted with FRP, and Hosotani and Kawashima (1999) and Youssef et al. (2007) proposed the design formulae of the lateral binding of rectangular and cylindrical columns and then suggested the formulae to predict the ultimate

*Correspondence: tw001@dankook.ac.kr
Department of Architectural Engineering, Dankook University, Yongin, Gyeonggi-do, Republic of Korea
Journal information: ISSN 1976-0485 / eISSN 2234-1315

strength and strain of retrofitted structures and the post -yield ductility.

These empirical formulae based on respective experiments were presented independently through previously conducted studies. Thus staff in actual sites may become confused in selecting proper formulae for respective applications; and accordingly, a comprehensive examination of the capability of the performance prediction of each formula is needed. In the meantime, the theory of neural networks which uses the human learning capability beyond the systematic learning of computers has been grafted onto recent engineering applications. The theory does not constitute the causal relationship of variables used for the design through functions, but, it predicts the results by exploiting the neural networks that consist of neurons, which are the basic elements involved in human perception and judgment. The system applied theory has been recently grafted onto the structural engineering applications (Imam et al. 2015, Lee et al. 2017), and rendered excellent predictive effects. For example, Gupta et al. (2006) and Kim et al. (2004) introduced the theory of neural networks that used the mixing ratio to estimate the compressive strength of concrete, and there is a case (Park 2006) that studied the reinforcement effect of concrete beams that employed the carbon fiber sheets for flexural reinforcement. In this study, the theory of neural networks that could imitate the human-decision making capability was applied to the prediction of the stress–strain relationship of concrete retrofitted with FRP.

That is, the basic physical properties that indicate the characteristics of fiber reinforcement, the coefficient representing the volume, and the conditions of test specimens to be retrofitted etc. were used as input variables to design the prediction system with fuzzy theory, which is the discipline belonging to the theories of neural networks, to predict the post-reinforcement strength (Ft), yield strain (εt), and post-yield elastic modulus (Eg) (see Fig. 1). The results obtained through experiments were applied to the prediction system to infer the predictability of the data needed for the reinforcement design with FRP. This study intended to build up a system that applied the fuzzy theory to predict the reinforcement effect of cylindrical compression retrofitted test specimens that were laterally bound with FRP.

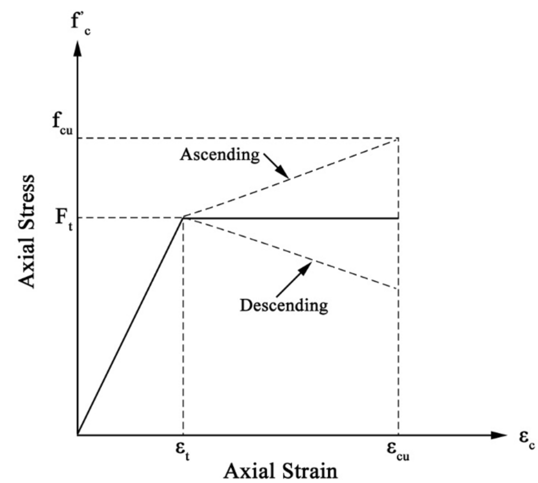

Fig. 1 Define of ascending and descending in Stress–strain relation.

2 Adaptive Neuro-Fuzzy Inference System

The Neural Network (Fukuda 1996) has been known as a representative method that imitates human learning capability, while the Fuzzy Theory is regarded as an alternative way to realize the human decision-making faculty. Recently, neuro-fuzzy techniques that imitate human learning and decision-making capability by combining neural network and fuzzy theories have been developed; and a neuro-fuzzy system like these techniques is introduced in this study. The neuro-fuzzy system is a fuzzy system that introduces the learning capability of neural network; and the combination of fuzzy logic system based on expert knowledge and introduced flexible learning capability is applied to problems that are unable to be solved with conventional concepts.

The fuzzy system (Gil and Park 1995) consists of an input membership function, fuzzy rule, and output membership function (Layer 5). The input membership function indicates Layer 1 that would be enumerated in the input space; and in this study, the reinforcement effect was defined as an influential element. The fuzzy rule is a combination of fuzzy inference concept and back propagation algorithm of neural network; and this also indicates the process of learning (Kim et al. 2004) that reaches the final value of designed neuro-fuzzy network having minimal error and the final objective value that is intended to be attained.

The Adaptive Network-based Fuzzy Inference System (ANFIS) having mixed learning rules (Cao et al. 1990) which was equipped to optimize parameters associated with the first Sugeno system (Kim 2003) was employed in this study. Figure 2 shows the configuration of the neuro-fuzzy system used in this study. The neuro-fuzzy system comprises 5 Layers: Layer 1 is assigned as an input node; Layers 2–4 indicate the process of applying the rule of fuzzy logic; and Layer 5 denotes the output layer. Here, both the input and output layers consist of two language layers. Each layer plays the following roles, and the output values of each Layer indicate the respective weighted values.

Layer 1 is a stage in which the parameters of membership function are determined.

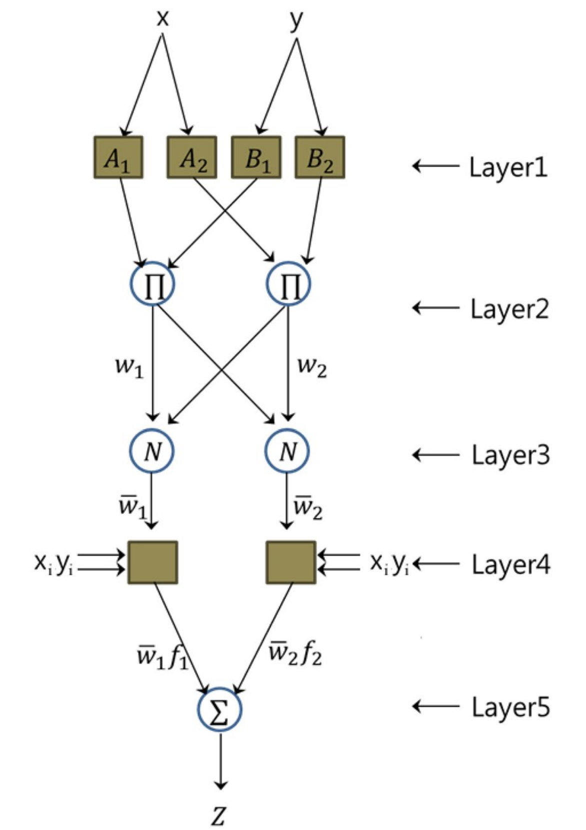

Fig. 2 Conceptual Organization of the ANFIS.

$$O_i^1 = \mu_{Ai}(x)\mu_{Ai}(x) = \exp\left\{-\left(\frac{x-c_i}{a_i}\right)^2\right\} \quad (1)$$

Here, the O_i^1 represents the membership function corresponding to each node at 'Level 1'; and x denotes the input value of each 'Node'. The c_i and a_i represent the membership function designed by the central value and value of standard deviation of the i-th input value at the first Layer 1. The parameter(s) of membership function is (are) determined at Layer 1 through the Eq. (1).

The Layer 2 generates the rule(s) and is a stage determining the degree of fulfillment of the generated rule(s). It can be represented as the following Eq. (2).

$$\omega_i = \mu_{Ai}(x) \times \mu_{Bi}(y), \quad i = 1,2 \quad (2)$$

In the figure above, the node implies the number of rules; and by calculating the fuzzy product using Eq. (2), the output of each node is represented as a strength of active function(s) of the rule(s).

Layer 3 is a stage that represents the degree of fulfillment of normalized rules, and the degree of fulfillment is expressed as the following Eq. (3).

Table 1 Prediction design for confined concrete using ANFIS.

CASE		Training set	Test set
1	Number of strength (F_t) data	284	16
2	Number of strain (ε_t) data	96	16
3	Number of Secondary elastic modules (E_g) data	87	16

$$\bar{\omega}_i = \frac{\omega_i}{\omega_1+\omega_2}, \quad i=1,2 \quad (3)$$

Layer 4 is a stage creating the final rule(s) that generates the output(s) as follows. The $\bar{\omega}_i$ is the value calculated at Layer 3; and f_i comprises the linear combination(s) to the input(s) as expressed in Eq. (4).

$$O_i^4 = \bar{\omega}_i f_i = \bar{\omega}_i(p_i x + q_i x + \nu_i) \quad (4)$$

Where, {pi, qi, ri} means the parameter set of final rule(s).

Layer 5 generates the final output(s) as represented in Eq. (5) by adding all input values output from Layer 4.

$$\boldsymbol{O_i^5} = \boldsymbol{z} = \sum_i \bar{\omega}_i \boldsymbol{f_i} = \frac{\sum_i \omega_i f_i}{\sum_i \omega_i} \quad (5)$$

Values input into the output layer will generate resulting output values if they are converged within the predetermined error rate; otherwise, they will be re-input into Layer 2 for reiterative calculation.

3 Prediction of Retrofitting Effects through the Neuro-Fuzzy System

3.1 Gaining of the Training Data

In this study, 284 data were collected through four research papers, which can identify the characteristics of reinforcing materials and the conditions of the base materials, in the existing researches that used FRP to reinforce the compression members, and the composition is shown in Table 1 (Lee et al. 2007; Lam and Teng 2002; Hwang 2001; Chun et al. 1999).

The 284 data (Case-1) represented the compressive strength (F_t), the 96 test specimens (Case-2) gave the information of strain (ε_t), and the 87 test specimens (Case-3) provided the information of Post Yielding Modulus(Eg) that were used to predict the effects of reinforcement; and the accuracy of prediction and applicability of the neuro-fuzzy system to the actual field were examined.

3.2 The Learning of Data

The data collected by each set were obtained from tests conducted according to test standards specified in KS F 2405 for the compressive strength test that employed the test specimens prepared with the dimensions of each of (diameter × height) of (100 × 200 mm) or (150 × 300 mm). The input variables for the learning of data were selected by using the design coefficients and conditions of the members to be retrofitted which were employed in existing studies that examined the reinforcement of the performance of structures by using the fiber reinforcement. That is, the compressive strength (f'c) of the concrete to be retrofitted, the thickness of reinforcement (tfrp), the number of layers of reinforcement, the elastic modulus of reinforcement (Efrp), the rupture strength of reinforcement (ffrp), the volumetric ratio of the reinforcement to concrete members to be retrofitted (K), and the dimensions of members (D, h) to be retrofitted etc. were selected as input layers; and the Ft, εt, Eg (see Fig. 3) were selected as output layers for the design of the neuro-fuzzy system.

The condition for the learning of data was designed by echo with the tolerance below 0.5%; and part of the

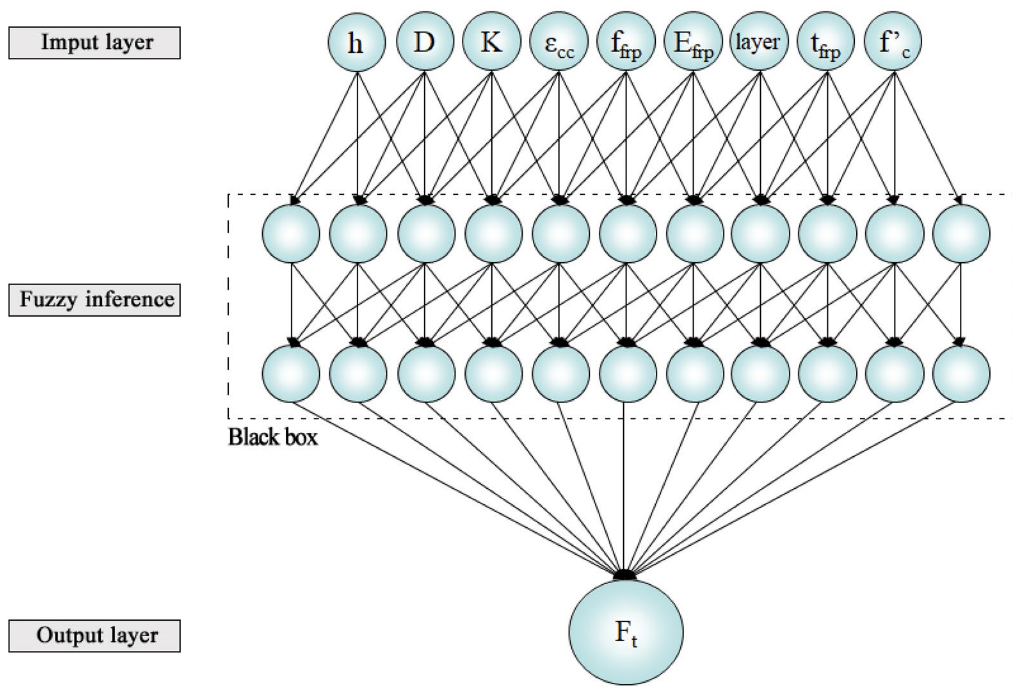

Fig. 3 Fuzzy design for CFRP retrofitting system.

Table 2 Samples for training data set in this study (part in 284 samples)

Data unit	f'_c MPa	t_{frp} cm	Layer ply	Kind –	E_{frp} GPa	f_{frp} MPa	ρ (%)	D cm	h cm	F_t MPa
1	38.6	0.031	1	G	73.3	755	0.816	15	31	45.5
2	30.2	0.017	1	A	224.6	2716	0.68	10	20	46.6
3	26.2	0.1	1	G	19.1	330	2.632	15	61	33.5
4	39.4	0.142	1	G	19.9	363	5.569	10	20	63.1
5	41.0	0.009	2	C	235	3500	0.706	5	10	117.0
6	45.2	0.011	2	C	230.5	3481	0.293	15	30	52.4
7	33.7	0.011	3	C	230.5	3481	0.440	10	20	109.9
8	35.0	0.08	3	G	36	560	2.105	15	44	83.0
9	43.7	0.0193	2	A	210	2173	0.772	10	20	88.0
10	33.28	0.0167	4	C	235	3550	0.668	10	20	111.1
11	20.79	0.0193	2	A	210	2173	0.772	10	20	72.8

t_{frp}: thickness of FRP; E_{frp}: young's modulus of FRP; ρ: Volume ratio; f_{frp}: ultimate strength of FRP; A: Aramid; G: Glass fiber; C: Carbon fiber.

data prepared for the learning of Case-1 (predictions of post reinforcement strength) were is represented in Table 2 to help understand the composition of data. The column without shade in Table 2 is the input layer, while the shaded column denotes the output layer representing the results of the predictions of post-reinforcement strength.

3.3 Distribution of the Data used for the Learning

Figure 4a illustrates the distribution of the data of maximum compressive strength (21.43–124.40 MPa, sorted in descending order) which were collected from existing studies to apply the fuzzy theory; Fig. 4b shows the strain at maximum compressive strength; and Fig. 4c represents the post-yield secondary elastic moduli sorted in descending order.

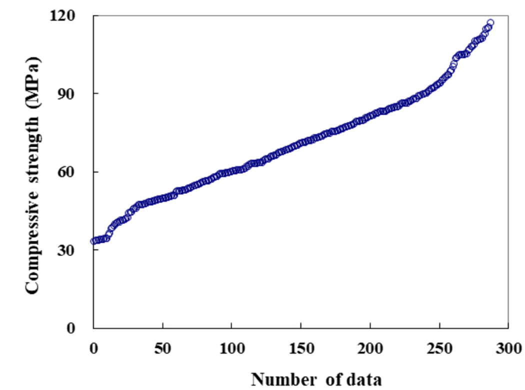

a Compressive strength

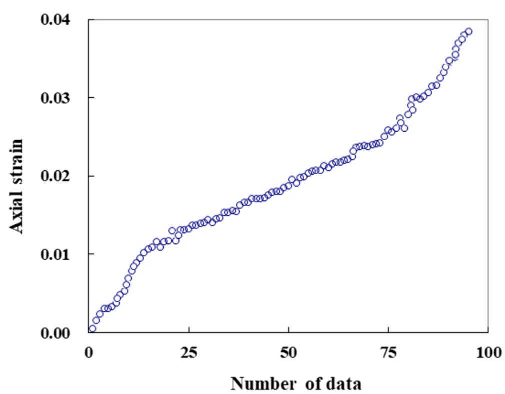

b Axial strain

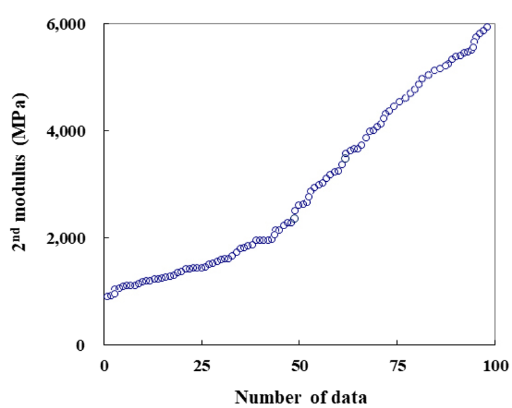

c 2nd Modulus

Fig. 4 Range of experimental values used as learning data.

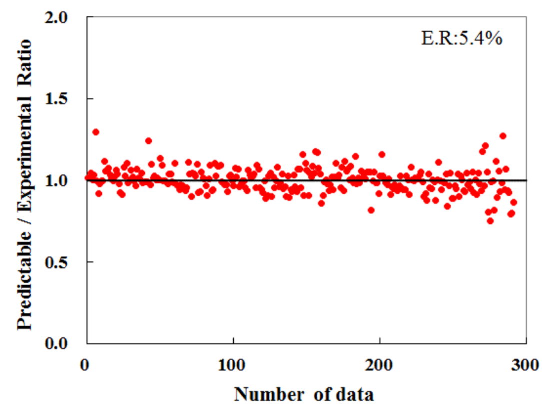

a Prediction ratio for strength in training stage

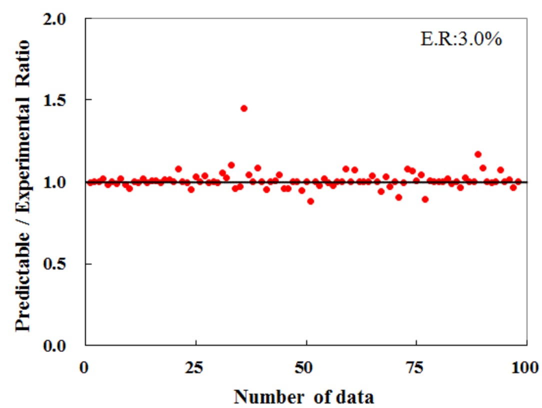

b Prediction ratio for strain in training stage

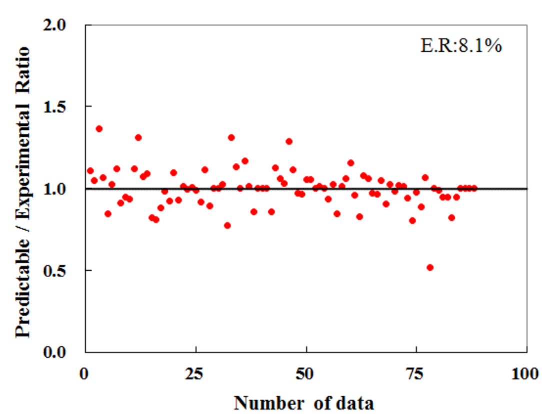

c Prediction ratio for 2nd modulus in training stage

Fig. 5 Prediction ratio in training stage.

3.4 Results of the Learning of Data

3.4.1 Results of the Learning

Figure 5a represents the results obtained from the learning of the neuro-fuzzy system conducted to predict the breaking strength of 284 cylindrical test specimens laterally bound with reinforcement fiber. The overall prediction error was 5.4% that appeared evenly in the interval of the distribution of predicted strength starting from the lower values to the higher ones.

Figure 5b illustrates the results with prediction error of 3.0% obtained from the neuro-fuzzy system applied to the prediction of axial strain of test specimens being broken, while Fig. 5c represents the results with prediction error of 8.1% rendered by the neuro-fuzzy system applied to the prediction of secondary post-yield elastic moduli of 87 cylindrical test specimens laterally bound with the reinforcement fiber.

$$E.R = \frac{abs(P.V - E.V.)}{E.V.} \times 100(\%) \tag{6}$$

where, P.V. means Predictable Value, and E.V. means Experimental Value

3.4.2 Statistical Examination

Figure 6 shows the histogram of the ratio of the resultant values obtained from the learning of the neuro-fuzzy system to the values obtained from tests conducted by the each data set of each model and the corresponding probability distribution functions for the statistical analysis.

Each model renders the shape of normal distribution; and that of Case-2 represents the highest probability distribution function. The values of the standard deviation were 0.075 (Case-1), 0.051 (Case-2), and 0.107 (Case-3); and the results show the lowest accuracy of the learning conducted to predict the secondary elastic moduli.

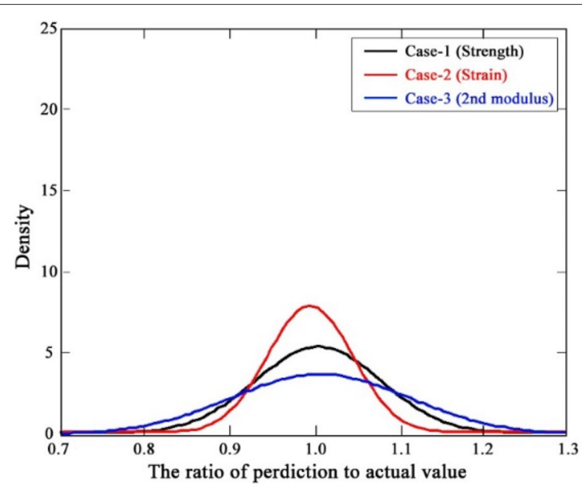

Fig. 6 Error ratio of prediction and actual data on statistical analysis.

Table 3 Results of the Statistical analysis.

	Case-1 (F_t)	Case-2 (ε_t)	Case-3 (E_g)
RMSE	4.79	0.00097	428.7
R^2	0.99889	0.99979	1.009
E.R	5.4	4.1	8.1

3.4.3 Analysis of Errors

The range of error was examined to assess the accuracy of learning of the neuro-fuzzy system. Equation (6) representing the percentage of error, the Root Mean Square Error (RMSE) representing the degree of error of predicted values, and the error of R2 (Absolute fraction of variation) representing the deviation of predictions from the test results were used to analyze the accuracy of learning of neuro-fuzzy system.

Table 3 shows the resultant errors of the learning of data in each Case, compared with the results obtained from each calculation of errors. The RMSE of the predicted strength in Case-1 was about ± 4.78 MPa, and that of Case-2 predicted the strain was 0.00096, while it was ± 428.66 MPa in Case-3. The values of R^2 representing the degree of deviation were 0.9957, 0.9982, and 0.9831 respectively showing the favorable level of learning.

3.4.4 Comparison of the Results of Learning with the Results Obtained from the Existing Formulae

Studies that delved into the prediction of stress & strain of laterally bound concrete to introduce the predictions into design have been conducted for a long time. Most of the prediction formulae developed through such studies were based on the regression analysis of the data obtained from respective tests. Youssef (2003) presented the stress–strain model through the test that employed cylindrical test specimens laterally bound with FRP, and proposed the stress prediction formula of retrofitted concrete as represented in the following Eq. (7) through regression analysis.

$$\frac{f_{cu}}{f'_c} = 1.0 + 2.25\left(\frac{f_{lu}}{f'_c}\right)^{\frac{5}{4}} \tag{7}$$

f’c: the compressive strength of concrete; fcu: the ultimate compressive strength of the test specimen retrofitted with FRP; flu: the effective strength of reinforcement at the ultimate compressive strength.

Figure 7 shows that the above expression applied to the data set used for the learning conducted in this study generates an error of about 24.8%. In particular, the expression did not predict the characteristics of strength in the domain beyond 90 MPa. Figure 8

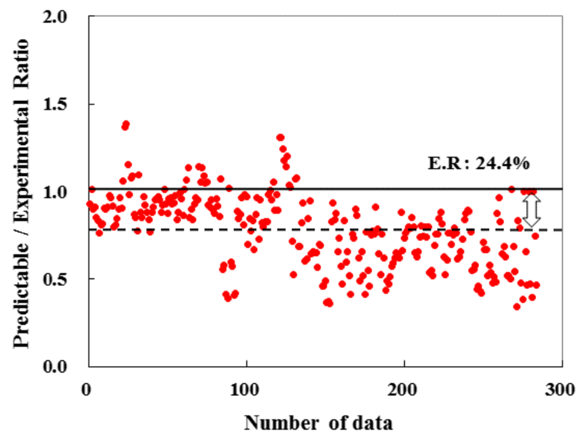

Fig. 7 Prediction ratio of confined concrete by Eq. (7).

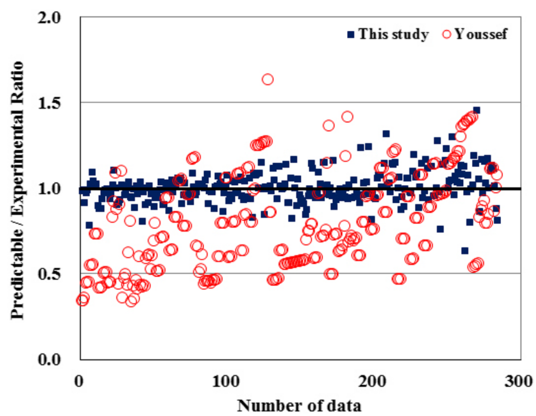

Fig. 8 Prediction ratio confined concrete between Youssef's research and this study.

illustrates the ratios of predictions of the case applied the neuro-fuzzy system designed in this study to those calculated by Eq. (7); and it represents the more precise predictions of the neuro-fuzzy system established in this study.

4 Verification of the Outputs of the Neuro-Fuzzy System

4.1 Design of Experiment and Preparation of Test Specimens

For the test to be conducted to verify the neuro-fuzzy system designed in this study, the 16 test specimens were prepared in the laboratory as represented in Table 4. The test specimens were made to the dimensions of the general test specimen (150 × 300 mm) and the extended one (150 × 600 mm; the length of four times of the diameter of the cylindrical test specimen) prepared for further tests conducted in this study to predict the reinforcement effects of cylindrical columns. The cylindrical mold form and the pipe made of PVC were used to make cylindrical test specimens to measure the compressive strength.

The mixing ratios of concrete used to make the test specimens were determined by the design strength of 21 MPa, as represented in Table 5. After the placement of concrete, all the test specimens were cured for 28 days in atmospheric condition, and the measured compressive strength was 20.1 MPa.

4.2 Reinforcement of Test Specimens

The test variables of test specimens to be employed for the test of reinforcement were determined to be identical to variables of the input layer for the learning of data; and the amount of reinforcement (ρ) was set by distinguishing the thickness and number of layers of each reinforcement. The surface of concrete was completely dried and treated before the reinforcement of test specimens, and the dust on the surface of concrete was removed by compressed air. Thereafter, the test specimens were coated with epoxy mortar in constant thickness, and the reinforcements were attached on each test specimen according to respective variables as shown in Fig. 9; both edges of test specimens were sheet-wrapped to prevent the breaking of the edges. Table 6 shows the physical properties of the reinforcement employed in this study.

4.3 The Test and Measurements

A Universal Testing Machine (UTM) of the capacity of 2000 kN was employed in the test. Test specimens were placed on the center of the loader by using auxiliary fittings made of iron that were fitted on the center of the loading frame, and the load cell was installed on each test specimen.

A hinge was inserted between the test specimen and loader to prevent eccentricity. A guide was installed on the upper and lower edges of the test specimen to measure the displacement of the test specimen; and displacement meters (LVDTs) of the precision of ± 25 mm were installed on the left and right edges of the test specimen to measure the axial displacement. Loading up to the 75% of expected load was carried out by applying load control, and thereafter the test specimen was loaded by strain control; and the results of the test were collected through a data collector (UCAM-5BT). Figure 10 shows a photo of the testing machine.

4.4 Results of the Test

The test specimens maintained high toughness by the reinforcement as shown in Fig. 11, and thereafter broke rapidly with the rupture of the reinforcement. The

Table 4 Summary of retrofitting specimen property.

Name	ρ (%)	Name	ρ (%)
H2-Ⅰ0	0.53	N2-Ⅰ0	0.27
H2-Ⅰ1	0.27	N2-Ⅱ3	0.27
H2-Ⅰ2	0.18	N3-Ⅱ1	0.8
H2-Ⅰ3	0.13	N3-Ⅱ3	0.4
H2-Ⅰ4	0.11	N3-Ⅰ1	0.4
H2-Ⅰ1-T	0.53	N3-Ⅰ1	0.8
H2-Ⅰ1-A	0.53	N3-Ⅰ0-A	0.8
H2-Ⅰ1-B	0.53	N3-Ⅰ1-B	0.8

H2 – Ⅰ 1 B

- Splice (T:0, A:240, B:480)
- Space (0:25, 1: 50, 2:75, 3:100, 4:125)
- Width (Ⅰ:25, Ⅱ:50)
- Thickness (2, 3)
- Size (Higher : 600, Normal : 300)

Table 5 Mix properties of concrete.

Design	Slump	W/C (%)	Mixture (kg/m^3)					
			C	W	S	G	Air	Admix
21 MPa	12 cm	54.7	328	180	865	950	4.5 ±1.5%	1.5

breakdown of the test specimen was initiated by cracking on the part of the bondage between the concrete and fiber reinforcement, followed by the rupture of reinforcement, and conical breakdown of the test specimen. Table 7 summarizes the results of the test.

4.5 Results of the Verification of the Neuro-Fuzzy System

In this study, 16 data as represented in Table 1 were used to verify the performance of the neuro-fuzzy system designed in the study. The data set used for the verification of the performance of the neuro-fuzzy system comprises the compressive strength of concrete to be retrofitted, the thickness of reinforcement, the number of layers of fiber reinforcement, the elastic modulus and rupture strength of the reinforcement, the volumetric ratio of the reinforcement to concrete, and the dimensions of members to be retrofitted, which were set as data for an input layer as the data set used for the learning of the neuro-fuzzy system, through which the compressive strength, strain, and post- yielding modulus of the output layer were estimated.

Fig. 9 Retrofitting process on H2-I1 specimen.

Figure 12 shows the results of the verification of the neuro-fuzzy system, which rendered errors of 11.5%, 7.5%, and 16.7% respectively. The case of the prediction of strength revealed superior predictions to those obtained from the method presented by Yossef thus it was judged that the established neuro-fuzzy system can be applied to predictions of the degree of reinforcement of the compressive strength of the retrofitted members.

Table 6 Properties of FRP.

Tensile strength (MPa)	Modulus of elasticity (GPa)
1991	158.2

Fig. 10 UTM (Capacity 2000 kN).

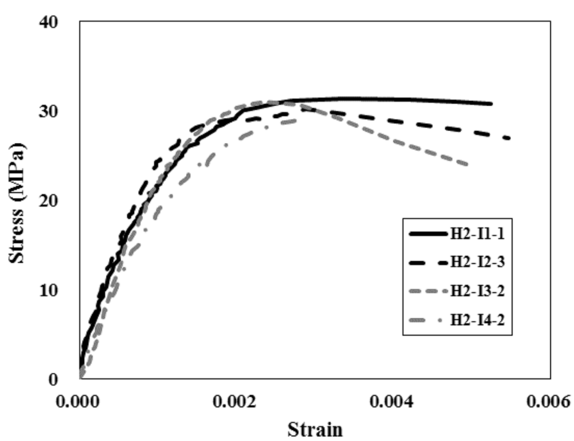

Fig. 11 Stress–strain relationship of H series.

5 Conclusions

This study intended to appraise the applicability of a neuro-fuzzy system to predict the stress–strain relationship of concrete members retrofitted with fiber reinforcement by using the data obtained through tests conducted in previous studies. The results obtained from this study are summarized as follow:

Table 7 Summary of the testing data.

Specimen	F_t (MPa)	ε_t	E_g (MPa)
H*	26.61	0.0023	− 25,974**
H2-I 0	32.63	0.003	12,810.59
H2-I 1	31.28	0.0033	2527.83
H2-I 2	30.67	0.0028	− 13,138.2**
H2-I 3	31.43	0.0027	− 24,890.9**
H2-I 4	30.48	0.0027	− 34,703.1**
H2-I 1-T	34.86	0.0032	11,652.96
H2-I 1-A	35.33	0.0037	5081.056
H2-I 1-B	37.02	0.0036	22,674.68
N*	21.13	0.0018	− 19,276.4**
N2-I0	25.70	0.0031	3156.05
N2-II3	26.66	0.0031	2852.00
N3-II1	26.83	0.0039	9814.00
N3-II3	25.87	0.0035	4602.43
N3-I1	26.57	0.0034	6210.99
N3-I1-T	29.07	0.0036	8967.37
N3-I0-A	28.59	0.00378	5697.24
N3-I1-B	29.81	0.0037	7984.13

*H and N are reference specimens.

**(−) symbol means 'descending' at Fig. 1.

(1) The compressive strength of concrete members to be retrofitted, thickness of reinforcement, number of reinforcing layers of reinforcement, elastic modulus of reinforcement, rupture strength of reinforcement, volumetric ratio of reinforcement to concrete members to be retrofitted, and dimensions of the concrete member to be retrofitted can be used as variables of the input layer of the learning of the neuro-fuzzy system to estimate the compressive strength, strain, and secondary modulus of elasticity of the retrofitted members of the output layer.

(2) The 284 data obtained from tests conducted in previous studies were employed as the data set for the learning of the adaptive neuro-fuzzy inference system (ANFIS) developed for this study, together with 16 test specimens retrofitted with fiber reinforcement to predict the effects of reinforcement. The results of the prediction of the effects of reinforcement showed errors of 11.5% for the predicted breaking strength, 7.5% for the predicted strain, and 16.7% for the predicted secondary elastic modulus.

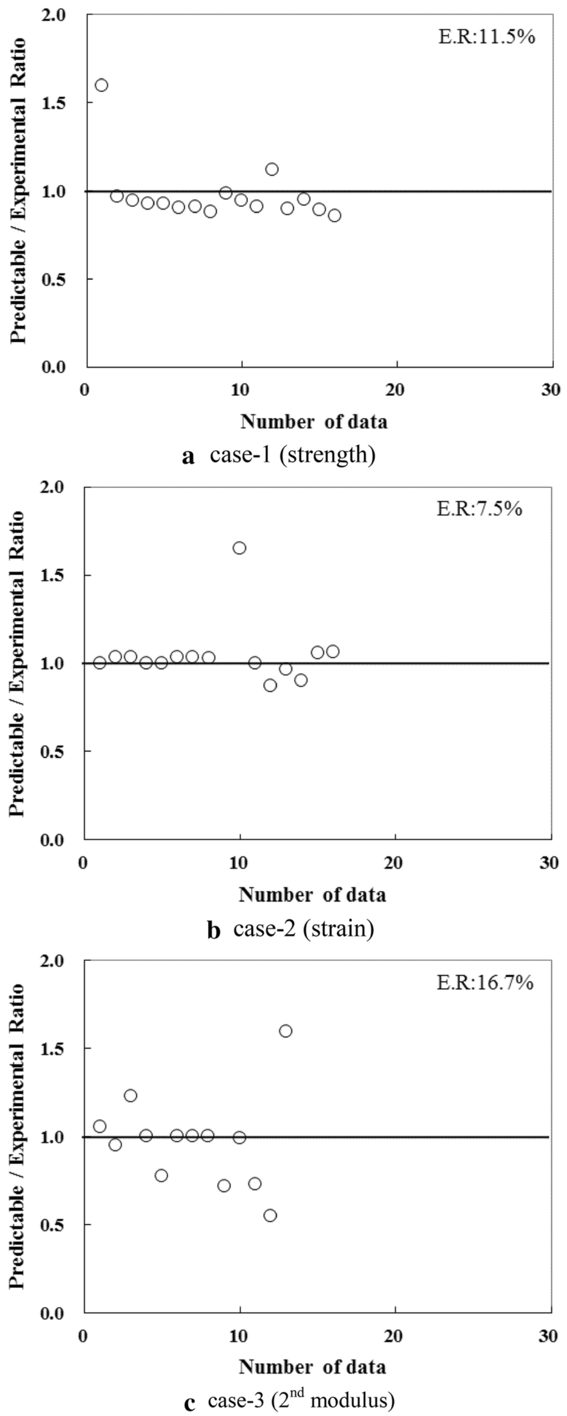

Fig. 12 Testing data diagram.

(3) An adaptive neuro-fuzzy inference system (ANFIS) was designed in this study to learn the data obtained from experiments using the test specimens prepared by dimensional ratios of the diameter and length of each test specimen of 1:2 and 1:4; and the performance of learning of the neuro-fuzzy system was verified through tests that rendered excellent predictions of the effects of fiber reinforcement. Thus it was estimated that the build-up of databases of actual members, such as columns or beams, would be desirable for further applications of this system.

Authors' Contributions

LC has designed this paper as a whole. He also applied a fuzzy algorithm to concrete specimens. TP performed the experimental study and wrote the paper. MH performed the analysis study. All authors read and approved the final manuscript.

Acknowledgements

The present research was conducted by the research fund of Dankook University in 2016.

Competing Interests

The authors declare that they have no competing interests.

Availability of Data and Materials

Not applicable.

Funding

Dankook University.

Publisher's Note

Received: 15 August 2018 Accepted: 10 October 2018
Published online: 29 December 2018

References

Al-Nimry, H., & Ghanem, A. (2017). FRP confinement of heat-damaged circular RC columns. *International Journal of Concrete Structures and Materials. KCI*, 11(1), 115–133.

Cao, Z., Kandel, A., & Li, L. (1990). A new model of fuzzy reasoning. *Fuzzy Sets and Systems, 36*, 311–325.

Cho, S. H. (2007). Stress–strain Responses of Concrete Confined by FRP Composites FRP. *Journal of the Korea Concrete Institute, 19*(6), 803–810.

Chun, S. C., Kim, J. Y., Park, H. C., & Park, C. L. (1999). Study on the stress–strain model of concrete confined by carbon fiber sheets. *Journal of Architectural Institute of Korea, 15*(1), 27–36.

Fukuda, H. (1996). Neural network and its application to structural engineering. *Journal of Korea Institute for Structural Maintenance and Inspection., 9*(3), 7–22.

Gil, J. M., & Park, D. H. (1995). Design of a Neuro—fuzzy inference engine and its applications. *Journal of Korea Institute for Structural Maintenance and Inspection, 22*(6), 868–879.

Gupta, R., Kewalramani, M. A., & Goel, A. (2006). Prediction of concrete strength using neural-expert system. *Journal of Materials in Civil Engineering ASCE, 118*(3), 462–466.

Hosotani, M., & Kawashima, K. (1999). A stress–strain model for concrete cylinders confined by both Carbon Fiber Sheets and Tie Reinforcement. *JSCE Journal of Concrete Engineering, 43*, 25–42.

Hwang, J. S. (2001). Stress–strain characteristics of the concrete cylinders confined by carbon fiber sheets. *Journal of Architectural Institute of Korea, 17*(2), 57–63.

Imam, A., Anifowose, F., & Azad, A. K. (2015). Residual Strength of Corroded Reinforced Concrete Beams Using an Adaptive Model Based on ANN. *International Journal of Concrete Structures and Materials, KCI*, *9*(2), 159–172.
Kim, Y. T. (2003). Independent joint adaptive control of robot manipulator using the sugeno-type of fuzzy logic. *Journal of the Korean Society for Precision Engineering, 20*(6), 55–61.
Kim, W. C., Choi, J. W., Kim, S. H., & Jang, M. S. (2004a). A study of the refined method of conflicts data with fuzzy-neural networks system. *Journal of the Korean Society of Civil Engineers., 24*(6), 839–844.
Kim, J. I., Kim, D. K., Feng, M. Q., & Yazdani, F. (2004b). Application of neural networks for estimation of concrete strength. *Journal of Materials in Civil Engineering, 16*(3), 257–264.
Lam, L., & Teng, J. G. (2002). Strength models for fiber-reinforced plastic-confined concrete. *Journal of structural engineering, ASCE, 128*(5), 612–623.
Lee, D. H., Kim, Y. S., & Jung, Y. S. (2007). Stress–strain Behavior Characteristics of Concrete Cylinders Confined with FRP Wrap. *Journal of the Korea Concrete Institute, 19*(2), 135–144.
Lee, C., Shin, S., & Lee, H. (2017). Balanced Ratio of Concrete Beams Internally Prestressed with Unbonded CFRP Tendons. *International Journal of Concrete Structures and Materials, KCI*, *11*(1), 1–16.
Mander, J. B., Priestley, M. J., & Park, R. (1988). Theoretical stress–strain model for confined concrete. *Journal of structural Engineering, ASCE, 114*(8), 1804–1826.
Park, D. K. (2006). Evaluation of the Bending Moment of FRP Reinforced Concrete Using Artificial Neural Network. *Journal of Korea Institute for Structural Maintenance and Inspection, 10*(6), 179–186.
Rechart, F. E., Brandtzaeg, A., & Brown, R. L. (1928). A study of the failure of concrete under confined compressive stress Bulletin 185 University of Illinois engineering experimental station Champion. *Bulletin, 185*, 85–88.
Youssef, M. N. (2003). Stress–strain model for concrete confined by FRP composites University of California Irvine, USA. *Composites: Part B, 38*, 614–628.
Youssef, Marwan N., Feng, Maria Q., & Mosallam, Ayman S. (2007). Stress–strain model for concrete confined by FRP composites. *Composites Part B Engineering, 38*, 614–628.